Chest CT Findings in Coronavirus Disease-19 (COVID-19): Relationship to Duration of Infection

Adam Bernheim, MD
Department of Diagnostic, Molecular and Interventional Radiology, Icahn School of Medicine at Mount Sinai, New York, NY

Xueyan Mei, MS
BioMedical Engineering and Imaging Institute, Icahn School of Medicine at Mount Sinai, New York, NY

Mingqian Huang, MD
Department of Diagnostic, Molecular and Interventional Radiology, Icahn School of Medicine at Mount Sinai, New York, NY

Yang Yang, PhD
Department of Diagnostic, Molecular and Interventional Radiology, Icahn School of Medicine at Mount Sinai, New York, NY

Zahi A. Fayad, PhD
Department of Diagnostic, Molecular and Interventional Radiology, and BioMedical Engineering and Imaging Institute, Icahn School of Medicine at Mount Sinai, New York,

Ning Zhang, MD
Department of Radiology, The First Affiliated Hospital of Nanchang University, NanChang, JiangXi, China

Kaiyue Diao, MD
Department of Radiology, West China Hospital, Sichuan University, Chengdu Sichuan, China

Bin Lin, MD
Department of Radiology, The Second Affiliated Hospital of Zhejiang University School Medicine, Hangzhou, China

Xiqi Zhu, MD
Department of Radiology, Nanxishan Hospital, Guangxi Zhuang Autonomous Region, China

Kunwei Li, MD
Department of Radiology, The Fifth Affiliated Hospital, Sun Yat-sen University, New Xiangzhou, Zhuhai, Guangdong Province, China

Shaolin Li, MD
Department of Radiology, The Fifth Affiliated Hospital, Sun Yat-sen University, New Xiangzhou, Zhuhai, Guangdong Province, China

Hong Shan, MD
Department of Radiology, The Fifth Affiliated Hospital, Sun Yat- sen University, New Xiangzhou, Zhuhai, Guangdong Province, China

Adam Jacobi, MD
Department of Diagnostic, Molecular and Interventional Radiology, Icahn School of Medicine at Mount Sinai, New York, NY

Michael Chung, MD
Department of Diagnostic, Molecular and Interventional Radiology, Icahn School of Medicine at Mount Sinai, New York, NY

Address correspondence to:
Adam Bernheim, MD
Assistant Professor, Department of Diagnostic, Molecular and Interventional Radiology, Icahn School of Medicine at Mount Sinai, New York, NY
1 Gustave Levy Place
New York, NY 10029
Email: adam.bernheim@mountsinai.org

Grants, Disclosures, or Other Assistance of Authors: None.
IRB Statement: IRB approval was waived for this study.

Abstract

In this retrospective study, chest CTs of 121 symptomatic patients infected with coronavirus disease-19 (COVID-19) from four centers in China from January 18, 2020 to February 2, 2020 were reviewed for common CT findings in relationship to the time between symptom onset and the initial CT scan (i.e. early, 0-2 days (36 patients), intermediate 3-5 days (33 patients), late 6-12 days (25 patients)). The hallmarks of COVID-19 infection on imaging were bilateral and peripheral ground-glass and consolidative pulmonary opacities. Notably, 20/36 (56%) of early patients had a normal CT. With a longer time after the onset of symptoms, CT findings were more frequent, including consolidation, bilateral and peripheral disease, greater total lung involvement, linear opacities, “crazy-paving” pattern and the “reverse halo” sign. Bilateral lung involvement was observed in 10/36 early patients (28%), 25/33 intermediate patients (76%), and 22/25 late patients (88%).

Introduction

An outbreak of coronavirus disease-19 (COVID-19) infection began in December 2019 in Wuhan, the capital of central China’s Hubei province [1, 2]. While the virus likely has a zoonotic origin related to the city’s Huanan Seafood Market, widespread human-to-human transmission has resulted in 73,451 cases in 26 countries with 1,875 deaths as of February 18, 2020 [3 - 7]. Disease was first reported in the United States on January 20, 2020, and the total number of cases in the United States has reached 15 as of February 17, 2020 [7, 8]. The most common presenting clinical symptoms are fever and cough in addition to other non-specific symptomatology including dyspnea, headache, muscle soreness, and fatigue [9]. About 20% of cases are severe, and mortality is approximately 3% [10]. The World Health Organization (WHO) declared a global health emergency on January 30, 2020 [11].

This is the seventh known coronavirus to infect humans [1]. Two other notable examples include severe acute respiratory syndrome (SARS) and Middle East respiratory syndrome (MERS), the former of which began in southern China and resulted in 774 deaths out of 8,098 infected individuals in 29 countries from November 2002 through July 2003, and the latter of which originated in Saudi Arabia and was responsible for 848 deaths among 2,458 individuals in 27 countries through July 2019 [12, 13].

As clinical physicians, epidemiologists, virologists, phylogeneticists, and others work with public health officials and policymakers to understand infection pathogenesis and control disease spread, some early investigators have observed imaging patterns on chest radiography and computed tomography (CT) [14 - 25]. For instance, an initial prospective analysis in Wuhan revealed bilateral lung opacities on 40 of 41 (98%) chest CTs in infected patients and described lobular and subsegmental areas of consolidation as the most typical findings [4]. Other investigators examined chest CTs in 21 infected patients and found high rates of ground-glass opacities and consolidation, sometimes with a rounded morphology and peripheral lung distribution [26]. Another group evaluated lung abnormalities related to disease time course and found that chest CT showed the most extensive disease approximately ten days after symptom onset. [16]. Thoracic radiology evaluation is often key to the evaluation of patients suspected of COVID-19 infection. Prompt recognition of disease is invaluable to ensure timely treatment, and from a public health perspective, rapid patient isolation is crucial for containment of this communicable disease.

In this study, we characterize chest CT findings in 121 patients infected with COVID-19 in China in relationship to the time between symptom onset and the initial CT scan. This study builds on initial work by early investigators during the first few weeks of the outbreak by evaluating a larger number of patients as well as by examining imaging features as the disease moves into the more subacute phase and/or earlier detection with increased vigilance for detection. We hypothesized that certain CT findings may be more common depending on the time course of infection.

Materials and Methods

Our institutional review board (IRB) waived written informed consent for this retrospective study that evaluated de-identified data and involved no potential risk to patients. To avert any potential breach of confidentiality, no link between the patients and the researchers was made available.

From January 18, 2020, until February 2, 2020, 121 adult patients admitted to four hospitals in four provinces in China with confirmed COVID-19 and who underwent chest CT were enrolled in our study. Twenty-one of these patients were previously evaluated on our prior study focusing on the CT imaging manifestations of COVID-19, but were reevaluated for the purposes of this

new study [26]. Patient selection was consecutive in each of the four institutions, and the solitary exclusion criteria was patient age < 18 years (Table 1). In addition to age and gender, clinical information collected included travel and exposure history (when known). All patients were positive for COVID-19 via laboratory testing with real-time reverse transcriptase polymerase chain reaction (rRT-PCR) of respiratory secretions obtained by bronchoalveolar lavage, endotracheal aspirate, nasopharyngeal swab, or oropharyngeal swab. In addition, the number of rRT-PCR tests performed on each patient was tabulated (when known), on which test a positive result was found was tabulated, and the number of days between symptomology onset and date of first positive test was tracked. The rRT-PCR test kits used on the patients in this study were manufactured by Sansure Biotech Inc. (Changsha, China), Shanghai Zhijiang Biotechnology Co. (Shanghai, China), or Da An Gene Co. (Guangzhuo, China).

Twenty-two patients were from Nanchang (Jiangxi Province) and were imaged with 8-mm slice thickness CT on a Siemens Emotion 16 scanner (Siemens Healthineers; Erlangen, Germany). Sixty-nine patients were from Zhuhai (Guangdong Province) and were imaged with 1-mm slice thickness CT on a UCT 760 scanner (United Imaging; Shanghai, China). Twenty-two patients were from Chengdu (Sichuan province) and were imaged with 1-mm slice thickness CT on a Revolution scanner (GE Medical Systems; Milwaukee, WI). Eight patients were from Guilin (Guangxi province) and were imaged with 1-mm slice thickness CT on a Philips Brilliance Big Bore scanner (Philips; Amsterdam, Netherlands). All scans were performed without intravenous contrast with the patient in the supine position during end-inspiration. Only the initial chest CTs were evaluated; if a patient had a follow-up CT during the study time window, it was not analyzed for this study.

All CT images were reviewed by two fellowship-trained cardiothoracic radiologists with approximately five years of experience each (A.B., M.C.) using a viewing console. Imaging was reviewed independently and final decisions reached by consensus are reported. No negative control cases were examined.

For each patient, the chest CT scan was evaluated for the following characteristics: (1) presence of ground-glass opacities, (2) presence of consolidation, (3) laterality of ground-glass opacities and consolidation, (4) number of lobes affected where either ground-glass or consolidative opacities were present, (5) degree of involvement of each lung lobe in addition to overall extent of lung involvement measured by means of a “total severity score” as detailed

below, (6) presence of nodules, (7) presence of a pleural effusion, (8) presence of thoracic lymphadenopathy (defined as lymph node size of ≥10 mm in short-axis dimension), (9) airways abnormalities (including airway wall thickening, bronchiectasis, and endoluminal secretions), (10) axial distribution of disease (categorized as no axial distribution of disease, central "peribronchovascular" predominant disease, or peripheral predominant disease), and (11) presence of underlying lung disease such as emphysema or fibrosis. Other abnormalities, including linear opacities, opacities with a rounded morphology, opacities with a "reverse halo" sign, opacities with a "crazy-paving" pattern, and opacities with intralesional cavitation, were noted. Ground-glass opacification was defined as hazy increased lung attenuation with preservation of bronchial and vascular margins, whereas consolidation was defined as opacification with obscuration of margins of vessels and airway walls [27]. Each of the five lung lobes was assessed for degree of involvement and classified as none (0%), minimal (1 - 25%), mild (26 - 50%), moderate (51 - 75%), or severe (76 - 100%). No involvement corresponded to a lobe score of 0, minimal to a lobe score of 1, mild to a lobe score of 2, moderate to a lobe score of 3, and severe to a lobe score of 4. An overall lung "total severity score" was reached by summing the five lobe scores (range of possible scores, 0 - 20).

The amount of time between the initial appearance of patient symptoms (such as fever, cough, etc.) and the date of both the first positive rRT-PCR test as well as the date of the initial chest CT examination was noted for each patient. Twenty seven patients were excluded because the date of first symptom appearance was unknown, leaving 94 patients for analysis. If the time interval between first clinical symptom and CT was two days or less (36 of 94 patients), the patient was considered to have been imaged in the "*early*" phase of illness. If the time interval was between three and five days (33 of 94 patients), the patient was considered to have been imaged in the "*intermediate*" phase of illness. If the time interval was between six and 12 days (25 of 94 patients), the patient was considered to have been imaged in the "*late*" phase of illness.

Results

There were 61 men and 60 women studied with mean age 45.3 years (age range 18 - 80 years with standard deviation 16 years).

Of the 121 patients, 27 (22%) had no ground-glass opacities and no consolidation on chest CT (Table 2). Of the 94 patients with ground-glass opacities, consolidation, or both, 41 (34%) had

only ground-glass opacities (with no consolidation), and two patients (2%) had consolidation in the absence of ground-glass opacities. Eighteen patients (15%) had opacities in one lobe, 14 patients (12%) had two affected lobes, 11 patients (9%) had three affected lobes, 18 patients (15%) had four affected lobes, and 33 patients (27%) had disease affecting all five lobes.

The right upper lobe was involved in 53 of 121 patients (44%), the right middle lobe was involved in 50 patients (41%), the right lower lobe was involved in 79 patients (65%), the left upper lobe was involved in 58 patients (48%), and the left lower lobe was involved in 76 patients (63%). Seventy-three of 121 patients (60%) had bilateral lung disease (Figure 1). Twenty (17%) patients had exclusively unilateral lung involvement, including 13 patients that had only right lung involvement (Figure 2) and 7 patients that had only left lung involvement. The mean total lung severity score for the 121 patients was 3 (range 0 - 18 with standard deviation 3). Thoracic lymphadenopathy, lung cavitation, and pulmonary nodules were notably absent in all 121 patients, and only 1 patient (1%) had a pleural effusion (a trace left effusion) (Table 3).

The time between initial onset of symptoms and subsequent chest CT was known for 94 patients and assigned as early (0-2 days), intermediate (3-5 days), or late (6-12 days). The frequency of ground-glass opacities and consolidation was far fewer in the early group as compared with the intermediate and late groups (Table 4, Figures 3 and 4). Twenty of 36 early patients (56%, 95%CI 47-65%) had no lung opacities as compared with three of 33 intermediate patients (9%) and 1 of 25 (4%) late patients. Bilateral lung involvement was observed in 10 of 36 early patients (28%), 25 of 33 intermediate patients (76%), and 22 of 25 late patients (88%). The mean total severity score was 1 (standard deviation (SD) = 1) for early patients, 4 (SD=2), for intermediate patients and 6 (SD= 4) for late patients.

Linear opacities, a “crazy-paving” pattern, and a “reverse halo” sign were all absent in the early group, but were present in the late group 20%, 20%, and 4% of the time, respectively (Figure 5). In terms of distribution of disease in the axial plane, peripheral distribution was found in 8 of 36 early patients (22%), 21 of 33 intermediate patients (64%), and 18 of 25 of late patients (72%).

All patients eventually had positive rRT-PCR for Covid-19. Of the 121 patients in this study, the date of the first positive rRT-PCR test was known in 102 of patients. There were 90 of 102 (88%) positive on the first test, including 33/36 (92%) in the early group, 28/33 (85%) in the

intermediate group, and 23/25 (92%) in the late group. The mean number of days between symptom onset and first positive rRT-PCR result was 4.5 days for all 102 patients (range 0 – 18 days), 2.3 days for the early group (range 0 – 7 days), 4.7 days for the intermediate group (range 0 – 18 days), and 7.2 days for the late group (range 1 – 12 days).

Discussion

An average of 3,605 new cases of COVID-19 have been reported per day since our preliminary research was published on February 4, 2020 [7]. Just as clinicians are evaluating more suspected patients, radiologists are similarly interpreting more chest CTs in those suspected of infection. Chest CT is a vital component in the diagnostic algorithm for patients with suspected COVID-19 infection. Indeed, given the limited number of rRT-PCR kits in some centers and the possibility of false negative rRT-PCR results, the National Health Commission of the People's Republic of China has encouraged diagnosis based on clinical and chest CT findings alone [28]. In this study of 121 patients with confirmed Covid-19 infection, it is noteworthy that 20/36 (56%) of patients imaged 0-2 days ('early') after symptom onset had a normal CT with complete absence of ground-glass opacities and consolidation (as opposed to 3/33 [9%] of intermediate patients and 1/25 [4%] of late patients). Only one of these patients (who was in the early group) had an initially negative rRT-PCR result, suggesting that rRT-PCR is positive even in patients with normal chest CT. Chest CT therefore has limited sensitivity and negative predictive value early after symptom onset, and is thereby unlikely a reliable standalone tool to rule out COVID-19 infection.

Other findings of this work largely concur with early radiology investigative efforts [16] insofar as this pattern of ground-glass and consolidative pulmonary opacities, often with a bilateral and peripheral lung distribution, is emerging as the chest CT hallmark of COVID-19 infection. This pattern of disease, somewhat similar to that described in earlier coronavirus outbreaks such as SARS and MERS, also dovetails with the blueprint thoracic radiologists recognize as the archetypal response to acute lung injury whereby an initial (often infectious or inflammatory) acute insult causes ground-glass opacities that may coalesce into dense consolidative lesions, and then progressively evolve and organize in often a more linear fashion with predilection for the lung periphery (and somewhat with a "crazy" paving pattern or emergence of a "reverse halo" sign). The findings in this study, which highlight the increased frequency of such findings

as consolidation, bilateral disease, greater total lung involvement, linear opacities, a “crazy-paving” pattern, appearance of the “reverse halo” sign, and peripheral lung distribution in patients imaged with CT a longer time after symptomatology starts, represent the CT correlate for the underlying pathophysiology of the disease process as it organizes. Moreover, the notable absence of ancillary chest CT findings such as lymphadenopathy, pleural effusions, pulmonary nodules, and lung cavitation likewise are consistent with early case descriptions.

There are several limitations to our study. Firstly, some patients were unable to be included in the evaluation of infection time course because of incomplete clinical histories where the precise time of symptom onset was unknown. Furthermore, some patients may have received medical intervention once suspected or confirmed to have infection (perhaps antimicrobial therapy, fluid administration, or steroid therapy may affect chest CT findings), which was not accounted for in this work. In addition, there may have been a selection bias in these institutions in terms of which patients were imaged with CT. For instance, if more clinically ill patients were more likely to be imaged sooner or imaged at all, then this may have an impact on results (although the opposite effect was observed in this study whereby those with the most severe lung involvement had a longer time between symptom onset and CT scan).

Our investigative efforts have demonstrated that frequency of CT findings is related to infection time course. Our data largely concur with work by Pan et al that demonstrated preponderance of ground-glass abnormality in early disease, followed by development of crazy paving, and finally increasing consolidation later in the disease course [16]. Meanwhile, the outbreak is at a stage of evolving from the acute to a more subacute phase in many patients. Recognizing imaging patterns based on infection time course is paramount for not only understanding the pathophysiology and natural history of infection, but also for helping to predict patient progression and potential complication development. Eventually, as infection duration in a large number of patients extends from the acute and subacute phases to either a completely healed outcome or to a chronic phase in patients over the coming several weeks and months, future investigators may evaluate imaging findings in chronic patients. Such work could evaluate if long-term complications absent in this study (such as pleural effusions, empyema, lymphadenopathy, and lung cavitation) potentially arise.

References

1. Zhu N, Zhang D, Wang W, et al. A novel coronavirus from patients with pneumonia in China, 2019. *N Engl J Med* 2020 January 24 (Epub ahead of print), doi: 10.1056/NEJMoa2001017.

2. Tan WJ, Zhao X, Ma XJ, et al. A novel coronavirus genome identified in a cluster of pneumonia cases - Wuhan, China 2019-2020. *China CDC Weekly* 2020; 2:61-62.

3. Chan JF, Yuan S, Kok KH, et al. A familiar cluster of pneumonia associated with the 2019 novel coronavirus indicating person-to-person transmission: a study of a family cluster. *Lancet* 2020 January 24 (Epub ahead of print), doi: 10.1016/S0140-6736(20)30154-9.

4. Huang C, Wang Y, Li X, et al. Clinical features of patients infected with 2019 novel coronavirus in Wuhan, China. *Lancet* 2020 January 24 (Epub ahead of print), doi: 10.1016/S0140-6736(20)30183-5.

5. Phan LT, Nguyen TV, Luong QC, et al. Importation and human-to-human transmission of a novel coronavirus in Vietnam. *N Engl J Med* 2020 January 28 (Epub ahead of print), doi: 10.1056/NEJMc2001272.

6. Li Q, Guan X, Wu P, et al. Early transmission dynamics in Wuhan, China, of novel coronavirus-infected pneumonia. *N Engl J Med* 2020 January 29 (Epub ahead of print), doi: 10.1056/NEJMoa2001316.

7. “Situation Report - 28.” *World Health Organization*, World Health Organization, 17 Feb. 2020, https://www.who.int/docs/default-source/coronaviruse/situation-reports/20200217-sitrep-28-covid-19.pdf?sfvrsn=a19cf2ad_2.

8. Holshue ML, DeBolt C, Lindquist S, et al. First case of 2019 novel coronavirus in the United States. *N Engl J Med* 2020 (Epub ahead of print), doi: 10.1056/NEJMoa2001191.

9. Wang W, Tang J, Wei F. Updated understanding of the outbreak of 2019 novel coronavirus (2019-nCoV) in Wuhan, China. *J Med Virol* 2020 January 29 (Epub ahead of print), doi: 10.1002/jmv.25689.

10. Wang C, Horby PW, Hayden FG, Gao GF. A novel coronavirus outbreak of global health concern. *Lancet* 2020 January 24 (Epub ahead of print), doi: 10.1016/S0140-6736(20)30185-9.

11. Mahase E. China coronavirus: WHO declares international emergency as death toll exceeds 200. *BMJ* 2020 January 31 (Epub ahead of print), doi: 10.1136/bmj.m408.

12. Lam CW, Chan MH, Wong CK. Severe acute respiratory syndrome: clinical and laboratory manifestations. *Clin Biochem Rev* 2004; 25:121-132.

13. Azhar Ei, Hui DSC, Memish ZA, Drosten C, Zumla A. The Middle East Respiratory Syndrome (MERS). *Infect Dis Clin North Am* 2019; 33:891-905.

14. Phelan AL, Katz R, Gostin LO. The novel coronavirus in Wuhan, China: challenges for global health governance. *JAMA* 2020 January 30 (Epub ahead of print), doi: 10.1001/jama.2020.1097.

15. Nishiura H, Jung SM, Linton NM, et al. The extent of transmission of novel coronavirus in Wuhan, China, 2020. *J Clin Med* 2020 January 24 (Epub ahead of print), doi: 10.3390/jcm9020330.

16. Pan F, Ye T, Sun P, et al. Time course of lung changes on chest CT during recovery from 2019 novel coronavirus (COVID-19) pneumonia. *Radiology* 2020 February 13 (Epub ahead of print), doi: 10.1148/radiol.2020200370.

17. Xie X, Zhong Z, Zhao W, Zheng C, Wang F, Liu J. Chest CT for typical 2019-nCoV pneumonia: relationship to negative RT-PCR testing. *Radiology* 2020 February 12 (Epub ahead of print), doi: 10.1148/radiol.2020200343.

18. Fang Y, Zhang H, Xu Y, Xie J, Pang P, Ji W. CT manifestations of two cases of 2019 novel coronavirus (2019-nCoV) pneumonia. *Radiology* 2020 February 7 (Epub ahead of print), doi: 10.1148/radiol.2020200280.

19. Song F, Shi N, Shan F, et al. Emerging coronavirus 2019-nCoV pneumonia. *Radiology* 2020 February 6 (Epub ahead of print), doi: 10.1148/radiol.2020200274.

20. Ng M, Lee E, Yang J, et al. Imaging profile of the COVID-19 infection: radiologic findings and literature review. *Radiology Cardiothoracic Imaging* 2020 February 13 (Epub ahead of print), doi: 10.1148/ryct.2020200034.

21. Kong W, Agarwal P. Chest imaging appearance of COVID-19 infection. *Radiology Cardiothoracic Imaging* 2020 February 13 (Epub ahead of print), doi: 10.1148/ryct.2020200028.

22. Kay F, Abbara S. The many faces of COVID-19: spectrum of imaging manifestations. *Radiology Cardiothoracic Imaging* 2020 February 14 (Epub ahead of print), doi: 10.1148/ryct.2020200037.

23. Wu Y, Xie Y, Wang X. Longitudinal CT findings in COVID-19 pneumonia: case presenting organizing pneumonia pattern. *Radiology Cardiothoracic Imaging* 2020 February 13 (Epub ahead of print), doi: 10.1148/ryct.2020200031.

24. Liu T, Huang P, Liu H, et al. Spectrum of chest CT findings in a familial cluster of COVID-19 infection. *Radiology Cardiothoracic Imaging* 2020 February 13 (Epub ahead of print), doi: 10.1148/ryct.2020200025.

25. Li X, Zeng X, Liu B, Yu Y. COVID-19 infection presenting with CT halo sign. *Radiology Cardiothoracic Imaging* 2020 February 12 (Epub ahead of pringt), doi: 10.1148/ryct.2020200026.

26. Chung M, Bernheim A, Mei X, et al. CT imaging features of 2019 novel coronavirus (2019-nCoV). *Radiology* 2020 February 4 (Epub ahead of print), doi: 10.1148/radiol.2020200230.

27. Hansell DM, Bankier AA, MacMahon H, McLoud TC, Müller NL, Remy J. Fleischner Society: glossary of terms for thoracic imaging. *Radiology* 2008; 246:697-722.

28. Yijiu X. China's Hubei reports jump in new cases of COVID-19 after diagnosis criteria revision. National Health Commission of the People's Republic of China website. www.en.nhc.gov/cn/2020-02/13/c_76515.htm. Published February 13, 2020. Accessed February 17, 2020.

Tables

Table 1: Patient Characteristics

GENDER	All patients N = 121	Early* (0-2 days) N = 36	Intermediate (3-5 days) N=33	Late (6-12 days) N=25
Men	61 (50)	16 (44)	16 (48)	11 (44)
Women	60 (50)	20 (56)	17 (52)	14 (56)
AGE (YEARS)				
Mean	45	45	47	50
Range	18 - 80	19 – 79	22 – 75	22 – 80
Standard Deviation	15.6	15.1	14.8	16.3
EXPOSURE HISTORY				
Recent Travel to Wuhan	92 (76)	33 (92)	28 (85)	21 (84)
Exposure to Infected Patient	7 (6)	2 (6)	2 (6)	2 (8)
Unknown Exposure	22 (18)	1 (3)	3 (9)	2 (8)
SYMPTOMS				
Fever	74 (61)	22 (61)	26 (79)	23 (92)
Cough	58 (48)	19 (53)	21 (64)	15 (60)
Sputum Production	20 (17)	7 (19)	5 (15)	6 (24)
RT PCR testing				
Initial RT-PCR Positive	90/102 (88)	33/36 (92)	28/33 (85)	23/25 (92)
Any Positive RT-PCR	121/121 (100)	36/36 (100)	33/33 (100)	25/25 (100)
Mean Day RT PCR was positive after symptom onset	4.5 (range 0-18)	2.3 (range 0-7)	4.7 (range 0-18)	7.2 (range 1-12)

Note: Numbers in Parentheses are Percentages

*Early, intermediate and late refer to time from symptom onset to time of the chest CT scan

Table 2: Findings on Chest CT in 121 Patients

GROUND-GLASS OPACITIES AND CONSOLIDATION	
Absence of Both Ground-Glass Opacities and Consolidation	27 (22)
Presence of Either Ground-Glass Opacities or Consolidation	94 (78)
Presence of Ground-Glass Opacities without Consolidation	41 (34)
Presence of Ground-Glass Opacities with Consolidation	50 (41)
Presence of Consolidation without Ground-Glass Opacities	2 (2)
NUMBER OF LOBES AFFECTED	
0	27 (22)
1	18 (15)
2rad	14 (12)
3	11 (9)
4	18 (15)
5	33 (27)
More than 2 lobes affected	62 (51)
Bilateral Lung Disease	73 (60)
FREQUENCY OF LOBE INVOLVEMENT	
Right Upper Lobe	53 (44)
Right Middle Lobe	50 (41)
Right Lower Lobe	79 (65)
Left Upper Lobe	58 (48)
Left Lower Lobe	76 (63)
TOTAL LUNG SEVERITY SCORE	
Mean	3
Range	0 - 18
Standard Deviation	3

Note: Numbers in Parentheses are Percentages

Table 3: Imaging Characteristics on Chest CT in 121 Patients

OPACITY CHARACTERISTICS	
Linear Opacities	9 (7)
Rounded Morphology of Opacities	65 (54)
Lung Cavitation	0 (0)
“Crazy-Paving” Pattern	6 (5)
“Reverse Halo” Sign	2 (2)
OPACITY (AXIAL) DISTRIBUTION	
No Axial Lung Distribution	58 (48)
Central (Peribronchovascular) Distribution	0 (0)
Peripheral Distribution	63 (52)
AIRWAYS	
Bronchial Wall Thickening	14 (12)
Bronchiectasis	1 (1)
Airways Secretions	1 (1)
UNDERLYING LUNG DISEASE	
Pulmonary Emphysema	2 (2)
Pulmonary Fibrosis	0 (0)
OTHER FINDINGS	
Pulmonary Nodules	0 (0)
Pleural Effusion	1 (1)
Thoracic Lymphadenopathy	0 (0)

Note: Numbers in Parentheses are Percentages

Table 4: Findings on Chest CT in Patients Categorized by Infection Time Course

	Early 0-2 days (n = 36 patients)	Intermediate 3-5 days (n = 33 patients)	Late 6-12 days (n = 25 patients)
Ground-glass opacities	16 (44)	29 (88)	22 (88)
Consolidation	6 (17)	18 (55)	15 (60)
No Lung Opacities in Any Lobe	20 (56)	3 (9)	1 (4)
Lung Opacities in 1 Lobe	6 (17)	4 (12)	1 (4)
Lung Opacities in 2 Lobes	2 (6)	6 (18)	4 (16)
Lung Opacities in 3 Lobes	3 (8)	3 (9)	0 (0)
Lung Opacities in 4 Lobes	1 (3)	7 (21)	6 (24)
Lung Opacities in 5 Lobes	4 (11)	10 (30)	13 (52)
Bilateral Lung Involvement	10 (28)	25 (76)	22 (88)
Mean Total Severity Score	1	4	6
Linear Opacities	0 (0)	3 (9)	5 (20)
Rounded Opacities	14 (39)	22 (67)	15 (60)
Lung Cavitation	0 (0)	0 (0)	0 (0)
“Crazy-Paving” Pattern	0 (0)	1 (3)	5 (20)
“Reverse Halo” Sign	0 (0)	0 (0)	1 (4)
No Axial Lung Distribution	28 (78)	12 (36)	7 (28)
Central (Peribronchovascular) Distribution	0 (0)	0 (0)	0 (0)
Peripheral Distribution	8 (22)	21 (64)	18 (72)
Bronchial Wall Thickening	4 (11)	4 (12)	6 (24)
Bronchiectasis	0 (0)	0 (0)	1 (4)
Airways Secretions	1 (3)	0 (0)	0 (0)
Underlying Pulmonary Emphysema	1 (3)	0 (0)	1 (4)
Underlying Pulmonary Fibrosis	0 (0)	0 (0)	0 (0)
Pulmonary Nodules	0 (0)	0 (0)	0 (0)
Pleural Effusion	0 (0)	0 (0)	0 (0)
Lymphadenopathy	0 (0)	0 (0)	0 (0)

Note: Numbers in Parentheses are Percentages

Figures

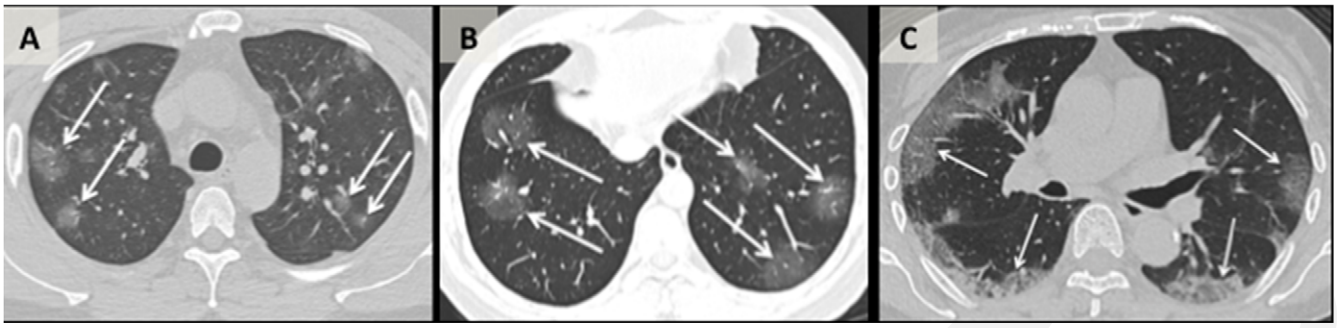

Figure 1:
An axial CT image obtained without intravenous contrast in a 36-year-old male (Panel A) shows bilateral ground-glass opacities in the upper lobes with a rounded morphology (arrows). An axial CT image obtained in a 44-year-old male (Panel B) shows larger ground-glass opacities in the bilateral lower lobes with a rounded morphology (arrows). An axial CT image obtained in a 65-year-old female (Panel C) shows bilateral ground-glass and consolidative opacities with a striking peripheral distribution.

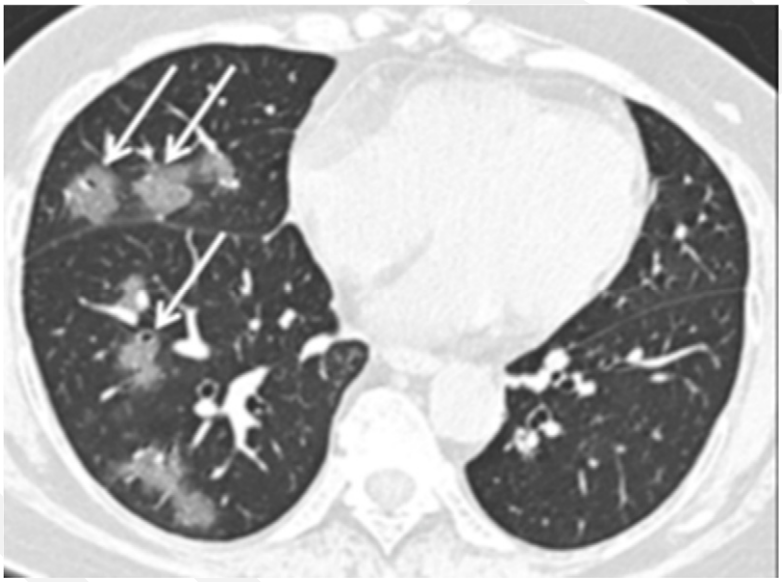

Figure 2:
An axial CT image obtained without intravenous contrast in a 56-year-old female shows ground-glass opacities with a rounded morphology (arrows) in the right middle and lower lobes. The left lung was normal.

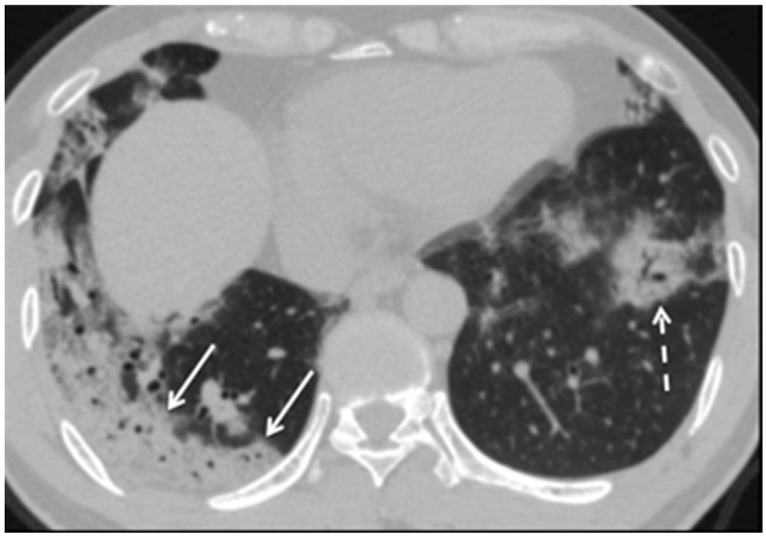

Figure 3:
An axial CT image obtained without intravenous contrast in a 42-year-old male in the "late" time group (10 days from symptom onset to this CT) shows bilateral consolidative opacities, with a striking peripheral distribution in the right lower lobe (solid arrows), and with a rounded morphology in the left lower lobe (dashed arrow).

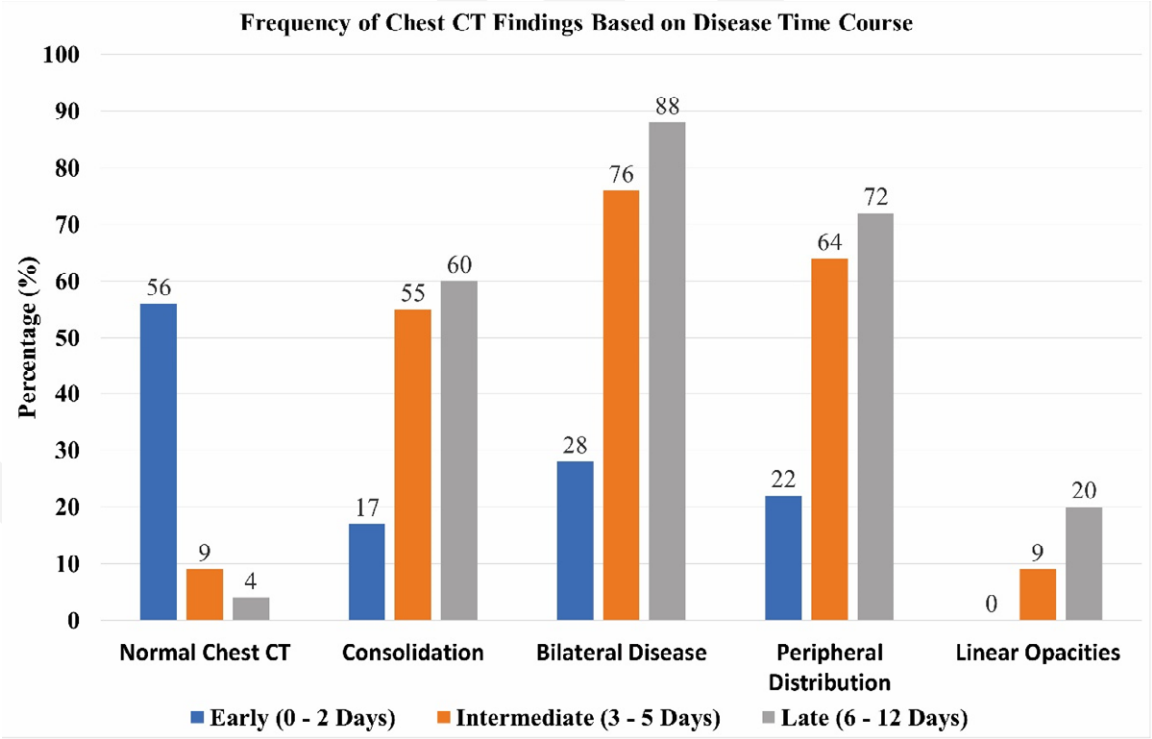

Figure 4:
Frequency of selected chest CT findings as a function of time course from symptom onset.

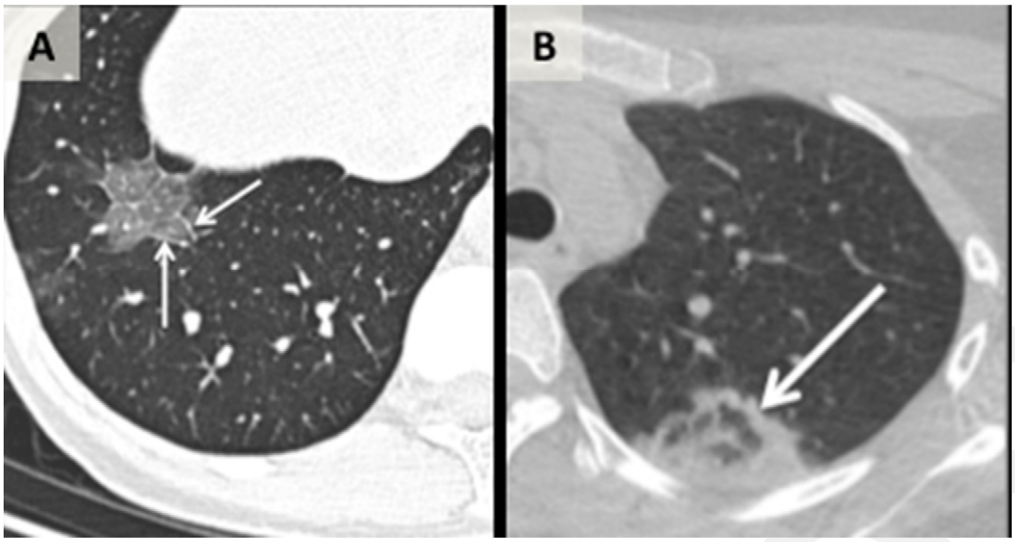

Figure 5:
An axial CT image obtained without intravenous contrast in a 43 year old female (Panel A) shows a "crazy-paving" pattern as manifested by right lower lobe ground-glass opacification with interlobular septal thickening (arrows) with intralobular lines. An axial CT image obtained in a 22-year old-female (Panel B) shows an area of faint ground-glass opacification in the left upper lobe with a ring of denser consolidation (arrow, "reverse halo" sign).